International Journal of Engineering

Electrophoretic Deposition of Microwave Combustion Synthesized Hydroxyapatite and Its Carbon Nanotube Reinforced Nanocomposite on 316L Stainless Steel

S. Rasouli[a], A. R. Gardeshzadeh*[a], M. Nabipour[b]

[a] *Department of Nanomaterials and Nanocoatings, Institute for Color Science and Technology, Tehran, Iran*
[b] *Islamic Azad University, Sciences & Research Branch, Hesarak, Tehran, .Iran; 1477893855*

P A P E R   I N F O

A B S T R A C T

Nanohydroxyapatite-carbon nanotube Nanocomposite (HA-CNT) coatings were deposited via electrophoretic deposition (EPD). Hydroxyapatite was synthesized via microwave combustion method using *calcium nitrate* and glycing as starting materials. X-ray diffraction (XRD) and Fourier transform infrared spectroscopy (FTIR) revealed that pure hydroxyapatite nanoparticles have been synthesized. AISI 316L stainless steel and ethanol were used as substrate and dispersing medium, respectively. 5%wt carbon nanotube (CNT) was used as reinforcing phase. Uniform and macrocrack-free coatings were obtained both for HA and *HA-5%wt CNT coatings*. Scanning electron microscopy (SEM) showed that most of microcracks in HA coating has eliminated after introducing CNT as reinforcing phase. The variation of deposit weight by time and voltage is measured both for HA and *HA-5%wt CNT* coatings. Thickness measurements indicated that for both coatings, the thickness increases with deposition voltage. X-ray diffraction patterns indicated that HA has not decomposed after sintering at 850 ˚C for 2 hr in argon atmosphere.

1. INTRODUCTION

Electrophoretic deposition (EPD) is a simple and low cost coating method which can be used for thick film deposition of ceramic materials [1, 2]. Recently, this technique has been used for deposition of hydroxyapatite $Ca_5(PO_4)_3OH$ (HA) coatings on biocompatible metals such as AISI 316L stainless steel [3-5], Ti [6, 7] and Ti-6Al-4V [8, 9] alloys for orthopedic applications. Wei et al. [10] deposited hydroxyapatite (HAp) coatings on substrates such as metallic biomaterials (Ti, Ti-6Al-4V, and 316L stainless steel) by electrophoretic deposition. They reported that metallic substrates tend to react with HA coatings at temperatures below 1050 ˚C, while decomposition for pure HA normally occurs above 1300˚C. Therefore, densification of these coatings needs to be conducted at temperatures lower than 1050 ˚C, and this necessitates the use of high-surface-area HA nano-precipitates. They also showed that the less equiaxed the nanoparticles,

more cracks initiate in the coatings obtained by the electrophoretic deposition technique.

The remarkable high mechanical strength and nanoscale morphology of CNTs make them attractive for biomedical applications, particularly for developing nanofibrous bioactive surfaces in combination with HA or bioactive glasses [11]. So, carbon nanotubes (CNT) are added to HA coatings to use mechanical properties of CNTs to reinforce HA layers obtained by EPD.

Both plasma spraying and laser surface treatment have been applied to produce HA/CNT composite layers on Ti–6Al–4V alloys [12, 13]. These two techniques however are cost-intensive coating technologies and it is also difficult to control the coating parameters and thickness during processing [12]. Kaya [14] deposited ultra-fine (20nm) hydroxyapatite powders-reinforced with multi-walled carbon nanotubes on Ti-6Al-4V medical alloy using electrophoretic deposition. He reported that the addition of carbon nanotubes increases hardness, elastic modulus and inter-laminar shear strength of monolithic hydroxyapatite layers. All of the investigations on electrophoretic deposition of CNT/hydroxyapatite coatings focused on Ti and especially Ti-6Al-4V as deposition substrate and

Corresponding Author Email: amirrg60@yahoo.com (A. R. Gardeshzadeh)

to our knowledge, there is not any report on electrophoretic deposition of CNT/hydroxyapatite coatings on 316L stainless steel substrates. The electrophoretic deposition of carbon nanotubes and its kinetic behavior in order to obtain a uniform coating as a cold cathode electrode in field emission devices is reported elsewhere [15, 16]. In this work, we investigated the deposition of nanohydroxyapatite and its carbon nanotube composite (HA- CNT) on 316L stainless steel substrates using EPD technique. The HA powder was synthesized by combustion method in microwave using glycine as fuel and calcium phosphate as starting material. The variation of deposit weight by deposition time and voltage as well as variation of film thickness by voltage are investigated. The phase stability of the coatings is also examined for both HA and HA-5%wt CNT coatings after sintering on 316L substrates.

2. EXPERIMENTAL

2. 1. HA Sysnthesis   Hydroxyapatite was synthesized via microwave combustion method. All the reagents were of analytical grade (Merck, Germany). A mixture of 5.1 g calcium nitrate and 3.7 g glycine was dissolved in 20 ml DI water using magnetic stirrer for 2 min. Ammonium was added dropwise in order to increase the pH from 6 to 9.5. At this time, pre-mixued phosphoric acid (1.1 ml) and ammonium (2.01 ml) was added to the mixture. Then nitric acid was added dropwise to reach the pH of 2. A viscouse gel was obtained after stirring the mixture for 30 min at 70 ˚C. The combustion reaction was performed using a 900 Watt microwave for 1 min. The obtained powder was then calcinated at 900 ˚C for 2 hr.

2. 2. Electrophoretic Deposition   Ethanol (Merck) used as dispersing medium. Multiwall carbon nanotube was purchased from PlasmaChem GmbH. The CNTs (purity>95%) were 1-10 micrometer in length and 5-20 nm in diameter. The SEM image of the as-received CNT is shown in Figure 1. 10 g/lit hydroxyl apatite suspension was prepared after sufficient ultrasonication. Then, 0.05 %wt iodine was added to enhance dispersability and particle surface charge. HA-5%wt CNT suspensions were also prepared for nanocomposite deposition after 10 min ultrasonication. EPD was performed under constant voltage using a DC power supply. AISI 316L atinless steel was sand blasted before

electrophoretic deposition. The chemical composition of the 316L stainless steel is presented in Table 1.

Deposit weight was measured using a 0.0001 balance. The deposition time was 3 min for all the experiments. 316L stainless steel substrates (4×4 cm^2) were sand blasted, acetone washed and dried in air for subsequent deposition.

After deposition, coatings were sintered at 850 ˚C for 2 h in argon atmosphere. In order to investigate decomposition of HA on the 316L substrate as well as in the presence of CNTs, The obtained coatings were characterized by X-ray diffraction (XRD) (Siemens, D500) after sintering. Scanning electron microscopy (SEM) micrographs were obtained on a LEO 1455VP scanning electron microscope. The thickness of the coatings were evaluated by Phynix digital thickness meter (± 1 μm), respectively.
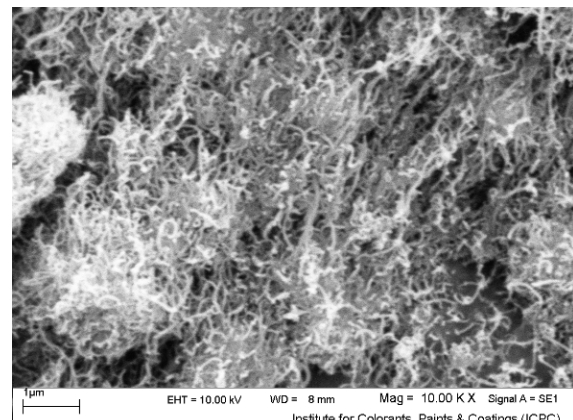

Figure 1. SEM images of the as-received CNT

3. RESULTS AND DISCUSSION

Figure 2 shows XRD and FTIR specra of the HA powder after calcination process. The XRD peaks correspond to hydroxyapatite phase (JCPDS No. 00-09-0432). In FTIR spectrum, the peaks at 3440 – 3640 cm^{-1} and 625-635 cm^{-1} correspond to the OH$^-$ vibrating bond. The peaks at 1045 cm^{-1} and 565-600 cm^{-1} are related to PO4$^-$ vibrating bond. Weak bonds of carbonate are also seen at 877 cm^{-1} and 1426 cm^{-1} which confirm substituting carbonate ions for phosphate ions. Scanning electron microscopy (SEM) image of the HA powder is shown in Figure 3.

TABLE 1. Chemical composition of 316L stainless steel used as deposition substrate.

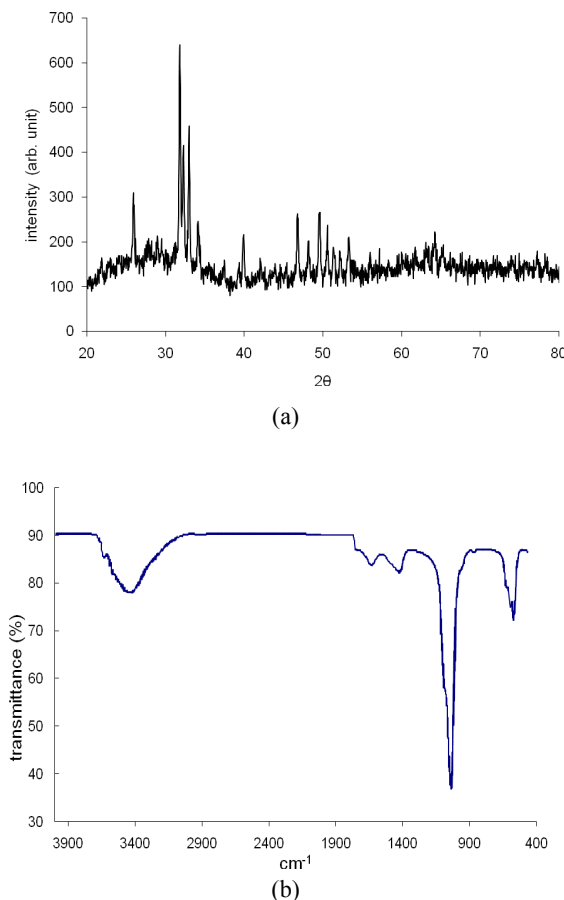| C	Si	Mn	P	S	Cr	Mo	Ni	Al	Co	Cu	Nb	Ti	V	W	Fe
0.028	0.35	1.35	0.04	0.003	16.90	2.23	10.50	0.004	0.13	0.28	0.007	Trace	0.028	0.03	base

(a)

(b)

Figure 2. (a) XRD and (b) FTIR specra of the synthesized HA powder after calcination at 900 ˚C for 2 h
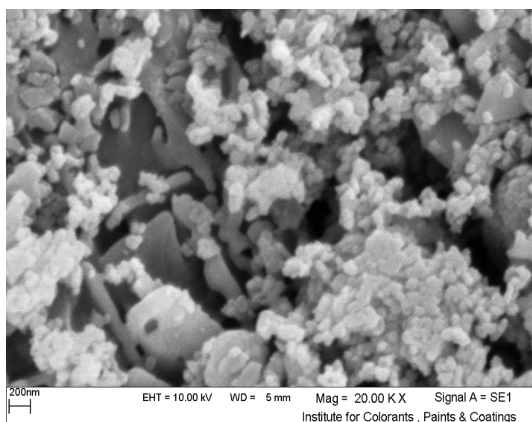

Figure 3. SEM micrograph of the as- calcined HA powder

Figure 4 shows macroimages of the deposited coatings. It is evident that there is no macrocrack in both obtained coatings, especially for HA-5%wt CNT. Comparing Figures 4a and 4b reveals that the

uniformity of the deposited coating has improved after introducing 5%wt CNT. This may be attributed to the simultaneous migration of HA and CNT particles and the ability of CNTs to fill the free spaces between HA nanoparticles, hence creating more uniform coatings after deposition. Figure 4 also shows the SEM images of the coatings after EPD process. It can be seen that in contrast to HA-5%wt CNT coating, there exists many microcracks in HA coating which will be detrimental to mechanical properties of final coatings. The existence of CNTs within the HA nanoparticles avoids the propagation of microcracks, so providing less-microcracked nanocomposites.

For investigating the electrophoretic behavior of these two coatings, the deposited weight (W) was measured at different times (t) and voltages (V). For all samples, the deposition area and the electrode distance were 4×3 cm^2 and 3 cm, respectively. For obtaining W-t curves (see Figure 5a), the deposited weight was measured after deposition at 100 V for 0.5, 1, 2, 3, 4 and 5 minutes. The W-V curves (see Figure 5b) were obtained after deposition at 50, 100, 200, 400 and 800 V for 3 minutes.

It can be seen from W-t curves that the deposition weight increases almost linearly with time. So, it is possible to predict the deposition weigh for other deposition times by interpolation or extrapolation. However, curve fitting was not successful in the case of W-V curves. It is evident from Figure 5b that at lower voltages, the increasing trend is nearly linear. But at higher voltages, there is a deviation from linear trend. This is because of the fact that at these voltages, more CNTs deposit on the surface at a given time, so the obtained coating has higher resistivity than those obtained at lower voltages. The resistivity lowers the deposition rate; hence the W-V curve deviates from the linear trend. Fluctuation and turbulence of the suspension also increases with the voltage which in turn, prevents CNTs from reaching the surface of the substrate. On the other hand, based on observations, some of the deposited coating removes from the surface during drawing the sample out of the suspension. Therefore, in this case, it is suggested to perform electrophoretic deposition at low to medium voltages (50-200 V) in order to obtain more uniform coatings.

Comparing the data obtained for HA and HA-5%wt CNT shows that in both W-t and W-V curves, the deposited weight for HA-5%wt CNT is lower than that of HA. This relates to the lower density of CNT in comparison with HA particles which results in a lightweight coating in the case of HA-5%wt CNT. These coatings are suitable for medical implants which need low weight coatings of hydroxyapatite.

The thickness of the HA and HA-5%wt CNT coatings was also measured after deposition at different

voltages (50, 100, 150 and 200 V) for 3 minutes. It can be seen from Table 2 that for both HA and HA-5%wt CNT coatings, the film thickness increases with deposition voltage. The obtained thickness ranges between 18-55 and 16-60 μm for HA and HA-5%wt CNT coatings, respectively. Each data is the average of five measurements on the surface of the samples. The standard deviation of the measured values for each sample is also listed in Table 2. The data confirm the uniformity of the coatings as was claimed in Figures 4a and 4b.

At a given voltage, the film thickness is approximately the same for HA and HA-5%wt CNT coatings. This shows that although HA-5%wt CNT coatings had lower weight, they exhibit the same thickness as HA coatings. Thus, it can be concluded that in the presence of CNTs, the thickness of the coatings has not changed considerably. In other words, CNTs has no undesirable effect on the thickness of the electrophoretic-deposited coatings.

Cross-section view of the HA and HA-5%wt CNT coatings deposited at 100 V and 3 min is shown in Figure 6. It can be seen that in HA cross section, some microcracks are visible, while the HA-5%wt CNT cross section is free of any microcracks. This is mainly attributed to the presence of CNT and its function as reinforcing phase. Hence, it can be concluded that it is possible to avoid crack formation in the electrophoretic deposited coatings by introducing as low as 5% carbon nanotubes to the matrix.

X-ray diffraction patterns of HA and HA-5%wt CNT coatings after sintering at 850 ˚C for 2 hr in argon atmosphere are shown in Figure 7. The peaks correspond to hydroxyapatite composition (JCPDS 01-070-0795) which confirms the chemical stability of the coatings on the 316L stainless steel after sintering.

It is well known that a typical carbon structure exhibits a XRD pattern consisting of a few broad bands located near the (002), (100), (110) and (112) reflections of graphite. In addition, the prominent peak about $2\theta= 26^o$ can be attributed to the (002) reflection of carbon [17]. However, in the case of HA-5%wt CNT sample, it seems that the peaks corresponding to CNT may either be overlapped by HA peaks or are not sufficiently intense. This is also reported by Najafi et al. [18] who investigated the inclusion of multi-walled carbon nanotubes as the second phase in the hydroxyapatite matrix via the sol–gel process. They pointed out that peaks at $2\theta = 26^o$ which were diverted to two branches, confirming the presence of CNT. It is also indicated that the HA phase is stable in the presence of CNTs. This means that CNTs had no detrimental effect on the HA matrix.
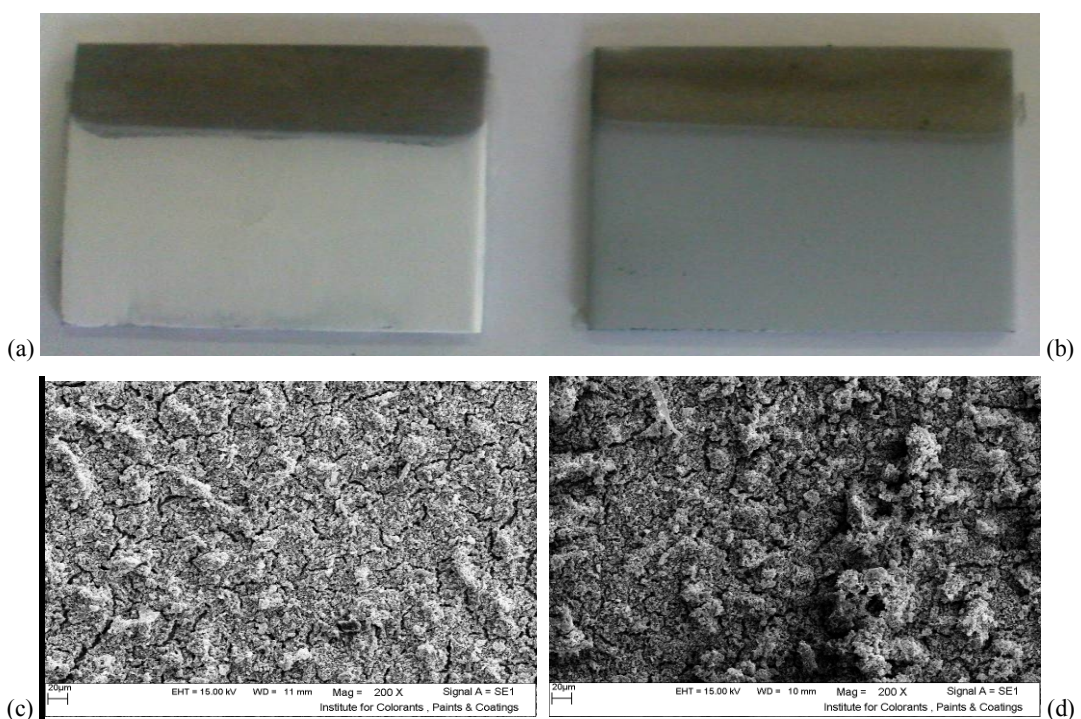

Figure 4. Macroimages of as deposited thick films: (a) HA and (b) HA-5%wt CNT coatings. Also shown SEM images of (c) HA, and (d) HA+CNT coatings.
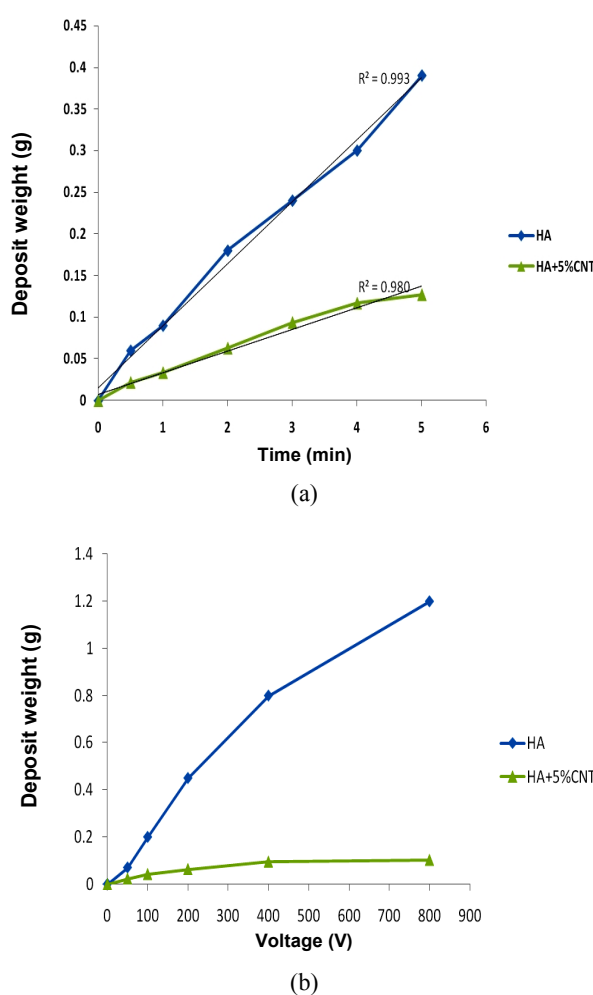
(a)

(b)

Figure 5. Variation of deposit weight by (a) deposition time and (b) electric field voltage for HA and HA-5%wt CNT coatings. The deposition area and the electrode distance are the same for all the samples (4×3 cm2 and 3 cm, respectively).

TABLE 2. Film thickness and the standard deviation measured for HA and HA-5%wt CNT coatings.

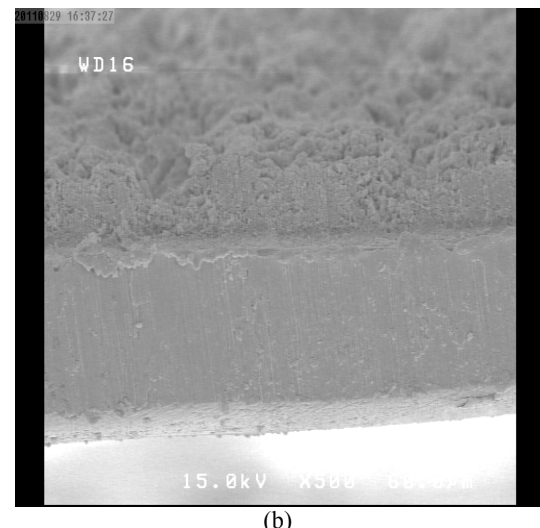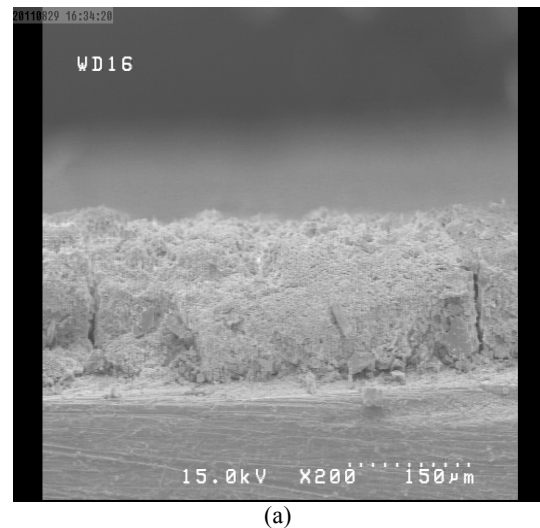| Sample	Deposition Voltage (V)	Thickness	Standard Deviation
HA	50	18.6	2.2
HA	100	48.6	2.6
HA	150	54.2	4.9
HA	200	55.6	4
HA+CNT	50	16	3.1
HA+CNT	100	45.4	4.2
HA+CNT	150	52.2	2.6
HA+CNT	200	59.3	2

(a)

(b)

Figure 6. SEM images from cross section of (a) HA and (b) HA-5%wt CNT coating deposited at 100 V and 3 min (500X).
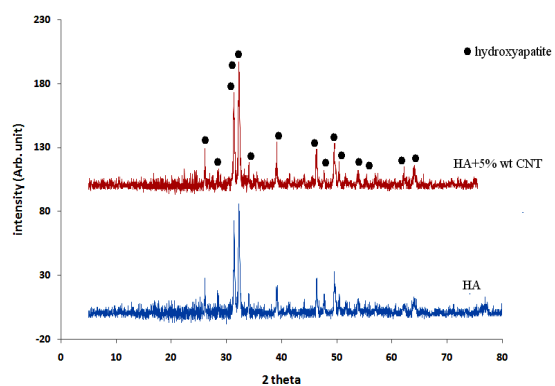

Figure 7. X-ray diffraction patterns of HA and HA-5%wt CNT coatings after sintering at 850 ˚C for 2 hr in argon atmosphere. All the peaks correspond to hydroxyapatite composition (JCPDS 01-070-0795)

4. CONCLUSIONS

1) HA nanoparticles were synthesized successfully by microwave combustion using glycine as the fuel.

2) HA and HA-5%wt CNT nanocomposites were deposited using EPD technique. It was shown that introducing 5%wt CNT into the HA results in a more uniform thick films with less surface microcracks which would improve the mechanical properties of the coatings.

3) The deposit weight increased almost linearly by deposition time, but it deviated from linear trend at high voltages (> 200 V). The deposit weight was much higher for HA coating in comparison with HA-5%wt CNT nanocomposites because of low density of CNTs compared with HA powder.

4) The thickness of both HA and HA-5%wt CNT coatings was in the range of 16-60 micrometer and increased with deposition voltage. The thickness values of HA and HA-5%wt CNT coatings were approximately the same at a given voltage. The thickness uniformity of the coatings was also desirable.

5) XRD analysis showed that HA was stable in the presence of CNTs and 316L stainless steel substrate after sintering.

6) Finally, it can be concluded that EPD is a promising technique for coating medical implants with HA and specially HA-CNT nanocomposites. As a result, uniform and lightweight coatings are attainable using low cost and simple apparatus.

5. REFERENCES

1. Corni, I., Ryan, M. P. and Boccaccini, A. R., "Electrophoretic deposition: From traditional ceramics to nanotechnology", *Journal of the European Ceramic Society*, Vol. 28, (2008), 1353–1367.

2. Boccaccinia, A. R. and Zhitomirsky, I., "Application of electrophoretic and electrolytic deposition techniques in ceramics processing", *Current Opinion in Solid State and Materials Science*, Vol. 6, (2002), 251-260.

3. Javidi, M., Javadpour, S., Bahrololoom, M. E. and Ma, J., "Electrophoretic deposition of natural hydroxyapatite on medical grade 316L stainless steel", *Materials Science and Engineering*, Vol. 28, (2008), 1509-1515.

4. García-Ruiz, G., Vargas, G., Méndez, N. J. and Uribe, S. A., "Water versus acetone electrophoretic deposition of hydroxyapatite on 316L stainless steel", *Key Engineering Materials*, Vol. 314, (2006), 237–244.

5. Sridhar, T. M., Kamachi Mudali, U., Subbaiyan, M., "Preparation and characterisation of electrophoretically deposited hydroxyapatite coatings on type 316L stainless steel", *Corrosion Science*, Vol. 45, (2003), 237–252.

6. Feng, Z. and Su, Q., "Electrophoretic deposition of hydroxyapatite coating", *Journal of Materials Science and Technology*, Vol. 19, (2003), 30-32.

7. Meng, X., Kwon, T. Y. and Kim, K. H., "Hydroxyapatite coating by electrophoretic deposition at dynamic voltage", *Dental Materials Journal*, Vol. 27, (2008), 666-671.

8. Kaya, C., "Electrophoretic deposition of carbon nanotube-reinforced hydroxyapatite bioactive layers on Ti-6Al-4V alloys for biomedical applications", *Ceramics International*, Vol. 34, (2008), 1843-1847.

9. Kwok, C. T., Wong, P. K., Cheng, F. T. and Man, H. C., "Characterization and corrosion behavior of hydroxyapatite coatings on Ti6Al4V fabricated by electrophoretic deposition", *Applied Surface Science*, Vol. 255, (2009), 6736-6744.

10. Wei, M., Ruys, A. J., Milthorpe, B. K. and Sorrell,C. C., "Precipitation of hydroxyapatite nanoparticles: Effects of precipitation method on electrophoretic deposition", *Journal of Materials Science Materials in Medicine*, Vol. 16, (2005), 319-324.

11. Boccaccini, A. R., Keim, S., Ma, R., Li, Y. and Zhitomirsky, I., "Electrophoretic deposition of biomaterials", *Journal of the Royal Society Interface*, Vol. 7, (2010), S581–S613.

12. Boccaccini, A. R., Choa, J., Subhani, T., Kaya, C. and Kaya, F., "Electrophoretic deposition of carbon nanotube–ceramic nanocomposites", *Journal of the European Ceramic Society*, Vol. 30, (2010), 1115-1129.

13. Kwok, C., "Fabrication of Carbon Nanotube Reinforced Hydroxyapatite Coating on Stainless Steel 316L by Laser Surface Treatment", *Towards Synthesis of Micro-/Nano-systems*, Part 2, Vol. B4, (2007), 261-265.

14. Kaya, C., "Electrophoretic deposition of carbon nanotube-reinforced hydroxyapatite bioactive layers on Ti-6Al-4V alloys for biomedical applications", *Ceramics International*, Vol. 34, (2008), 1843-1847.

15. Gardeshzadeh, A. R. and Raissi, B., "Thick film deposition of carbon nanotubes by alternating electrophoresis", *Progress in Color Colorants and Coatings*, Vol. 3, (2010), 27-31.

16. Gardeshzadeh, A. R. and Rasouli, S., "Kinetic Investigation of Carbon Nanotube Deposition by DC Electrophoretic Technique", *Progress in Color Colorants and Coatings*, Vol. 4, (2011), 51-58.

17. Stamatin, I., Morozan, A., Dumitru, A., Ciupina, V., Prodan, G., Niewolski, J. and Figiel, H., "The synthesis of multi-walled carbon nanotubes (MWNTs) by catalytic pyrolysis of the phenol-formaldehyde resins", *Physica E*, Vol. 37, (2007), 44–48.

18. Najafi, H., Nemati, Z. A. and Sadeghian, Z., "Inclusion of carbon nanotubes in a hydroxyapatite sol–gel matrix", *Ceramics International*, Vol. 35, (2009), 2987–2991.

Electrophoretic Deposition of Microwave Combustion Synthesized Hydroxyapatite and Its Carbon Nanotube Reinforced Nanocomposite on 316L Stainless Steel

S. Rasouli[a], A. R. Gardeshzadeh[a], M. Nabipour[b]

[a] Department of Nanomaterials and Nanocoatings, Institute for Color Science and Technology, Tehran, Iran
[b] Islamic Azad University, Sciences & Research Branch, Hesarak, Tehran, .Iran; 1477893855

چکیده

پوشش های نانوکامپوزیتی نانوهیدروکسی آپاتیت- نانولولـه کربنـی بـا روش لایـه نشـانی الکتروفـورتیکی تهیـه شـدند. هیدروکسی آپاتیت به روش احتراق مایکروویو با استفاده از مواد اولیه نیترات کلسیم و گلایسین سنتز شد. پراش پرتـوی ایکس و طیف بینی فروسرخ تبدیل فوریه نشان دادند که نانوذرات هیدروکسی آپاتیت خالص حاصل شده اند. فولاد زنگ نزن AISI 316L و اتانول بترتیب به عنوا زیرلایه و حلال مورد استفاده قرار گرفت. پوشش های HA و HA-5%wt CNT هـر دو یکنواخـت و بـدون ماکروترک بودند. میکروسکوپ الکترونی روبشی نشان داد که بعد از اضافه کردن نانولوله کربنی به عنوان فاز تقویت کننده، بخش زیادی از میکروترک ها حذف شده اند. تغییر وزن نشست با زمان ولتاژ برای هر دو پوشش اندازه گیری شد. اندازه گیری ضخامت نشان داد که در هر دو پوشش، ضخامت با ولتاژ لایه نشانی افزایش می یابد. الگوهای پراش پرتوی ایکس نشان دادند که بعد از سینتر در دمای ۸۵۰°C به مدت ۲ ساعت در محیط آرگون، هیدروکسی آپاتیت پایدار بـاقی مانـده است.